Banded Convective Activity and Ducted Gravity Waves

R. S. LINDZEN[1] AND K.-K. TUNG

Center for Earth and Planetary Physics, Harvard University, Cambridge, Mass. 02138

(Manuscript received 7 June 1976, in revised form 13 September 1976)

ABSTRACT

Convective activity is frequently organized into band-like structures with space and time scales appropriate to internal gravity waves. When the convective activity involves cumulonimbus, then latent heat release can form a significant energy source for the waves which in turn may organize the convection [as described, for example, by wave-CISK (Lindzen, 1974; Raymond, 1975)]. However, in other cases strong forcing is absent and the existence of the waves requires the existence of a duct from which very little wave energy leaks. We show that the energy cannot be contained by an inversion. Instead, we find that a stable duct adjacent to the surface must be capped by an unstable layer wherein the mean flow at some level either equals or comes close to the phase speed of the ducted waves. We also find that the wind amplitudes associated with the observed pressure amplitudes in these waves are consistent with observed squall winds. Finally, we find that the horizontal scales of mesoscale waves are closely related to the time scales of convective elements.

1. Introduction

It has often been noted that cumulus activity is frequently organized in banded structures which are characterized by horizontal wavelenghs of from about 100–400 km and travel relative to the mean flow with a phase speed of about 10–30 m s^{-1} (SESAME[2] 1974). A recent study of this phenomenon in the central United States was presented by Uccellini (1975). Similar structures are noted in the tropics, while cases for New England have recently been analyzed by Marks (1975). In some of these situations virtually the entire depth of the troposphere is conditionally unstable and surface air is warm and moist. [Almost all tropical cases fall into this category as do some of the midwest results presented by Uccellini (1975).] In such cases, latent heat released in cumulonimbus appears capable of efficiently forcing the waves which in turn serve to organize the cumulonimbus convection. We shall refer to such interactions generally as wave-CISK (Conditional Instability of the Second Kind). Specific examples of how such interactions produce gravity waves are given in Lindzen (1974) and Raymond (1975). There are, however, other cases where convection is restricted to upper levels, precipitation is small and the lower troposphere is stable [e.g., the Salem, Ill. case of Uccellini (1975), those of Marks (1975), and also that of Eom (1975)]. Such situations do not lend themselves to the wave-CISK mechanism; nevertheless the waves are observed to last for three to ten cycles. It is this latter class of waves that we will be considering in this paper. The problem in such cases is that waves of the observed wavelengths and phase speeds can propagate vertically freely, and hence, in the absence of the thermal forcing provided by CISK, they would lose their energy through vertical propagation before traveling even a single wavelength horizontally. This was noted, for example, in the SESAME (1974) Project Development Plan.

Traditionally, such waves have been presumed to be "waves on an inversion." This identification is based on the well-known existence of horizontally propagating waves along an interface between fluids of different densities in a two-layer fluid of finite depth and was exploited for meteorological purposes by Tepper (1950). Unfortunately, the two-layer fluid model differs profoundly from the atmosphere in two crucial respects: 1) the individual layers are unstratified and hence do not allow vertical propagation, and 2) the free upper surface is energy-containing and hence does not allow energy loss from the system. Thus, the identification of the atmospheric mesoscale waves as "waves on an inversion" seems, on the whole, unjustified. It will be the purpose of this paper to investigate under what circumstances such waves can exist in the atmosphere.

Briefly, we find that such waves can exist if a stable lower troposphere is bounded by a region above, which effectively reflects the vertically propagating waves, thus creating a duct wherein the waves may propagate horizontally without great loss of energy and hence without the need for energetic forcing. Our main con-

[1] Alfred P. Sloan Foundation Fellow.

[2] Severe Environmental Storms and Mesoscale Experiment Project Development Plan.

cern will be to determine what could provide such a reflecting surface. However, in Section 2 we will first hypothesize that such a surface exists and show how the phase speed of ducted waves is related to both the thickness and stability of the duct. (Indeed, there will in principle be an infinitude of ducted modes—each with a different phase speed; our primary interest is in the lowest mode whose horizontal phase speed is the greatest.) The precise nature of the surface will not significantly alter the results of Section 2. Although the results of Section 2 are very elementary, they serve to emphasize our contention that the phase speed of such waves depends on the gross properties of the duct rather than on the details of some interfacial discontinuity. In Section 2 we also investigate the meaning of ducted modes when the upper level is not a perfect reflector.

In Section 3 we investigate whether an inversion might not play some role in such waves—by serving as a reflecting surface. A brief consideration of the data suggests that this is unlikely since most observed inversions bound regions too thin to sustain the observed phase speeds. Our calculations confirm this, showing that any reasonable inversion is a poor reflector except for high order modes having very slow horizontal phase speeds [$O(1\ m\ s^{-1})$]. Such modes, for several reasons, are of little practical interest. In Section 4 we investigate the possibility that a conditionally unstable saturated layer could serve as a reflecting lid on a stable duct. Following a suggestion by Lalas and Einaudi (1974) we take the stability of such a layer to be some mean of the dry and saturated stabilities, which may be zero or even somewhat negative. Such layers will tend to trap vertically propagating gravity waves, and we find that, for observationally reasonable layer thicknesses, the reflectivity of such layers is significantly greater than that of inversion layers. However, for observed phase speeds, such layers provide insufficient reflectivities to allow the lower duct mode to be well defined and sufficiently long lived. This matter is investigated using the technique developed by Lindzen and Blake (1972). A qualitive consideration of the wave equations when a basic shear is present suggests that the reflectivity will be greatly enhanced if the conditionally unstable layer contains a critical (or steering) level where the flow speed equals the phase speed of the wave. We show, in Section 5, that this is in fact the case. In Section 6 we show that the reflectivity of such a layer can be large even if the mean flow does not quite reach the phase speed of the wave or when it does so slightly *above* the conditionally unstable layer. (A steering level *below* the unstable layer should destroy the duct.)

The work of Sections 2–6 leaves us with clear conditions for the existence of mesoscale waves when CISK is not relevant. A comparison with data for such cases (in Section 7) shows that our conditions do appear to be met. Several questions remain. First, is it reasonable to consider trapping by unstable layers? We believe it is, since the most rapidly growing instabilities are usually tightly confined to the unstable region and typically have a horizontal scale of the same order as the vertical scale of the unstable layer, while the waves we are concerned with have much longer horizontal scales. Second, why do the mesoscales exist at all? In Section 8, we present a suggestion which we believe is of considerable generality, namely, that when an unstable layer is adjacent to a stable duct, the instabilities in the unstable layer will stochastically perturb the stable duct with a spectrum of periods. If there is to be any collective interaction between waves in the stable duct and the instabilities, the shortest period at which such interactions can take place must be $O(2\pi\tau_i)$, where τ_i is the time scale of the instabilities. In the case of wave-CISK, Lindzen (1974) showed that this would be the preferred period. We suggest that similar considerations may lead to the selection of the same period in the present case. It is this preferred period, together with the characteristic phase speed of the stable duct, that determines the primary horizontal scale of the waves in the duct, which will in turn perturb the unstable region and tend to pattern the convection. Comparison with available tropospheric data appears completely consistent with these relations, and the applications of the same simple concept to the solar chromosphere seems to adequately predict the observed scale of supergranules.

2. Wave equations and properties of a duct

In this section, we investigate the properties of waves in a duct (which must be stable). For the convenience of presentation, an incompressible Boussinesq atmosphere will be used here, though we shall extend the results to the case of a compressible atmosphere later in this section.

The governing equations are

$$\left.\begin{aligned}\left(\frac{\partial}{\partial t}+U_0\frac{\partial}{\partial x}\right)u'+w'\frac{d}{dz}U_0&=-\frac{1}{\rho_0}\frac{\partial}{\partial x}p'\\ \left(\frac{\partial}{\partial t}+U_0\frac{\partial}{\partial x}\right)w'&=-\frac{1}{\rho_0}\frac{\partial}{\partial z}p'-\frac{g\rho'}{\rho_0}\\ \frac{\partial}{\partial x}u'+\frac{\partial}{\partial z}w'&=0\\ \left(\frac{\partial}{\partial t}+U_0\frac{\partial}{\partial x}\right)\rho'+w'\frac{d\rho_0}{dz}&=0\end{aligned}\right\},\qquad(1)$$

where u', w' are the perturbation velocities in the horizontal (x) direction and vertical (z) directions, respectively; ρ' and p' are the perturbation density and pressure; $\rho_0(z)$ is the mean density; and $U_0(z)$ the mean horizontal velocity. Assuming that the solu-

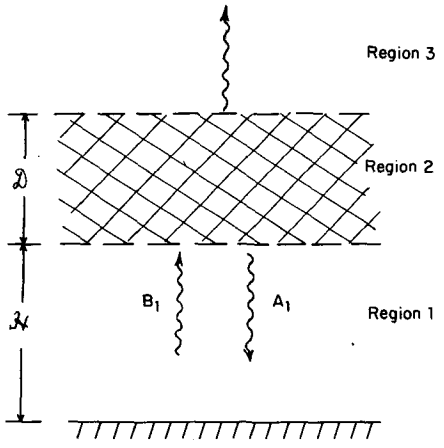

FIG. 1. Schematic diagram of the model atmosphere. Region 1 is the wave duct, region 2 the "black box" reflector, and region 3 is a semi-infinite propagating region.

tions are of the form $w' = w(z)e^{ik(x-ct)}$, etc., one obtains

$$\frac{d^2}{dz^2}w+\left[\frac{N^2}{(U_0-c)^2}-\frac{\frac{d^2}{dz^2}U_0}{(U_0-c)}-k^2\right]w=0, \qquad (2)$$

where $N^2 = (g/\rho_0)(d\rho_0/dz)$ is the Brunt-Väisälä frequency squared. Eq. (2) is the so-called Taylor-Goldstein equation.

Consider a wave duct (Fig. 1, region 1) bounded below by a lower boundary and above by an as yet unspecified "black box" reflector (Fig. 1, region 2). Let $C_D = c - U_1$ be the phase speed of the wave relative to the mean flow $U_0 = U_1$ in the duct. Both C_D and N^2 are assumed to be constant in region 1. The solution to Eq. (2) can be written as

$$w_1(z)=A_1\exp[i\lambda_1(z-\mathcal{H})]+B_1\exp[-i\lambda_1(z-\mathcal{H})], \qquad (3)$$

where $\lambda_1^2=(N_1^2/C_D^2)-k^2$ (λ_1 assumed positive). If C_D is taken to be positive (without loss of generality), then $B_1\exp[-i\lambda_1(z-\mathcal{H})]$ represents an upgoing (incident) wave, and $A_1\exp[i\lambda_1(z-\mathcal{H})]$ represents the reflected wave. We now define the reflection coefficient $\mathcal{R}$ to be

$$\mathcal{R}=\left|\frac{A_1}{B_1}\right| \qquad (4)$$

so that we can write

$$A_1=\mathcal{R}e^{i\theta}B_1, \quad |\theta|\leqslant\pi, \qquad (5)$$

where θ, real, is the phase shift. Note that, as far as the waves in the duct are concerned, $\mathcal{R}$ and θ contain all the information of the "outside world" (i.e., regions 2 and 3). Solution (3) can now be written as

$$w_1(z)=w_0\{\mathcal{R}\exp[i\lambda_1 z-i(2D-\theta)] +\exp[-i\lambda_1 z]\}/\{1+\mathcal{R}\exp[-i(2D-\theta)]\}, \qquad (6)$$

where $D=\lambda_1\mathcal{H}=2\pi\mathcal{H}/\mathcal{L}$, $\mathcal{L}$ being the vertical wavelength of the wave in the duct and w_0 the vertical velocity at the lower boundary $z = 0$. w_0 may be viewed as a forcing, and we see that forced waves may exist for any $\mathcal{L}$. By "free" oscillation we mean those solutions which exist when $w_0=0$.

Nontrivial free solutions exist only if the denominator in (6), vanishes. However, for an imperfect duct (i.e., $\mathcal{R}\neq 1$), it can be shown that the denominator never vanishes. As a consequence we have the obvious result that free waves do not exist in an imperfect duct. Thus, in the following we will be concerned only with waves that are "almost free." By that we mean wave modes that have a pronounced response for a given forcing [compare them with "free" waves, which exist in the absence of forcing or, in other words, give *infinite* responses in the presence of finite forcings (see Lindzen and Blake, 1972)].

We use, as a measure of "response," the amplitude of the surface pressure perturbation.[3]

$$\frac{p(0)}{\rho_0}=-\frac{C_D}{ik}\frac{d}{dz}w\Big|_{z=0}$$
$$=-\frac{C_D\lambda_1}{k}w_0\{\mathcal{R}\,e^{-i(2D-\theta)}-1\}/\{\mathcal{R}\,e^{-i(2D-\theta)}+1\}.$$

If we let

$$I\equiv\left|\frac{p(0)}{\rho_0 w_0}\right|,$$

then

$$I=\frac{C_D\lambda_1}{k}\left[\frac{\epsilon^2+2(1-\epsilon)[1-\cos(2D-\theta)]}{\epsilon^2+2(1-\epsilon)[1+\cos(2D-\theta)]}\right]^{\frac{1}{2}}, \qquad (7)$$

where $\epsilon\equiv 1-\mathcal{R}$.

It can be seen from (7) that if the reflector is not too far from being perfect (i.e., $\epsilon^2\ll 1$) the response will have pronounced peaks with amplitude

$$I\approx\frac{2C_D\lambda_1}{k}\frac{1}{|\epsilon|}, \qquad (8)$$

whenever

$$[1+\cos(2D-\theta)]=0. \qquad (9)$$

Eq. (9) gives the following quantization for the modes:

$$\mathcal{H}/\mathcal{L}_n+\theta/(4\pi)=\tfrac{1}{4}+\tfrac{1}{2}n, \quad n=0, 1, 2, \ldots, \qquad (10)$$

where $\mathcal{L}_n$ is the vertical wavelength of the nth mode. In the explicit cases we will consider, it usually turns out that θ is a small quantity, i.e., $|\theta/\pi|\ll 1$. Thus Eq. (10) can be written approximately as

$$\mathcal{H}/\mathcal{L}_n=\tfrac{1}{4}+\tfrac{1}{2}n, \quad n=0, 1, 2, \ldots. \qquad (11)$$

[3] It should be noted that with few exceptions, the exact choice of forcing or response measure is arbitrary and of no significance in the determination of "almost free modes."

The wave with the longest vertical wavelength is the $n=0$ mode. A quarter of its wavelength fits the thickness of the duct, i.e., $\frac{1}{4}\mathfrak{L}_0=\mathfrak{H}$. For other modes, $\mathfrak{H}$ is always an odd multiple of quarter wavelengths. In theory, all of the infinitude of such waves can exist in a stable duct. However, the higher order modes, having shorter space scales and relatedly slower phase speeds, ought to be more significantly attenuated by any dissipative processes; thus we expect the $n=0$ mode, whose vertical wavelength is longest, should dominate.

The phase speeds associated with the modes given by (11) can also be calculated. For waves with long horizontal wavelengths (viz., mesoscale waves),

$$\mathfrak{L}_n \approx 2\pi C_{D,n}/N_1. \tag{12}$$

Thus

$$C_{D,n} \approx \frac{N_1 \mathfrak{H}}{\pi(\frac{1}{2}+n)}, \quad n=0, 1, 2, \ldots. \tag{13}$$

Note that C_D, as given by Eq. (13), is independent of k. We see that the duct selects the phase speed of the wave, but not its horizontal scale. The horizontal wavelength is to be selected by other means, which shall be discussed in Section 8.

The following summarizes the properties necessary for a duct:

1) The duct has to be statically stable, i.e., N_1^2 has to be positive, so that wave propagation is possible in the duct.

2) The duct has to be sufficiently thick so that it can accomodate a quarter of the vertical wavelength corresponding to the observed phase speed. For example, suppose the observed phase speed of a mesoscale wave is $C_D \approx 25$ m s^{-1}, then the vertical wavelength can be deduced [from Eq. (12)] to be $\mathfrak{L}_0 \approx 12$ km. Therefore the duct has to have a thickness of at least 3 km. If the atmospheric condition is such that the stable region is appreciably less than 3 km thick, we can expect that this atmosphere does not have a duct that can support a 25 m s^{-1} mesoscale wave.

3) The duct has to be topped above by a good reflector. If the reflector is poor, wave energy will be rapidly lost through leakage by vertical radiation. We call a reflector a good one if it can reflect enough wave energy to sustain the wave for at least two cycles against leakage. For the longest wave ($n = 0$ mode), this requires that the reflector has a reflection coefficient $\mathcal{R}$ of at least 85% (see Appendix).

4) Finally, we must also note that the wind speed in the duct cannot be equal to the phase speed of the wave. If this occurs, a critical level would be situated in a *stable* region with Richardson number $>\frac{1}{4}$. Waves will then be totally absorbed (Booker and Bretherton, 1967).

Before concluding this section, we will briefly redevelop our results for a compressible atmosphere. The governing equations for a compressible hydrostatic atmosphere[4] in log-pressure coordinates are

$$\left.\begin{aligned} \left(\frac{\partial}{\partial t}+U_0\frac{\partial}{\partial x}\right)u'+w^{*\prime}\frac{d}{dz^*}U_0 &= -\frac{\partial}{\partial x}\Phi' \\ \frac{\partial}{\partial x}u'+\left(\frac{\partial}{\partial z^*}-1\right)w^{*\prime} &= 0 \\ \left(\frac{\partial}{\partial t}+U_0\frac{\partial}{\partial x}\right)\Phi_{z^*}'+w^{*\prime}S &= 0 \end{aligned}\right\}, \tag{14}$$

where $z^*=\ln[p_0(0)/p]$ is the log-pressure coordinate. $w^{*\prime}=Dz^*/Dt$ is the vertical velocity in z^* coordinate; it is related to the real vertical velocity w' through

$$Hw^{*\prime} = -\left(\frac{\partial}{\partial t}+U_0\frac{\partial}{\partial x}\right)(\Phi'/g)+w', \tag{15}$$

where $H=RT_0/g$ is the scale height of the atmosphere, $T_0(z)$ being the temperature of the basic state. We have defined in (14) the stability parameter

$$S=R\left(\frac{d}{dz^*}T_0+\frac{R}{c_p}T_0\right)=RH\Gamma,$$

where $\Gamma\equiv(1/H)(dT_0/dz^*)+(g/c_p)$ is the lapse rate of the atmosphere. The equations in (14) can be combined to give

$$\frac{d^2}{dz^{*2}}\tilde{w}+\left[\frac{S}{(U_0-c)^2}-\frac{\frac{d^2}{dz^{*2}}U_0+\frac{d}{dz^*}U_0}{(U_0-c)}-\frac{1}{4}\right]\tilde{w}=0, \tag{16}$$

where we have written

$$w^{*\prime}=\tilde{w}e^{-z^*/2}e^{ik(x-ct)}, \quad \text{etc.}$$

In the duct where U_0 and S are assumed constant, the solution to (16) is

$$\tilde{w}_1(z^*)=A_1e^{i\nu_1(z^*-h)}+B_1e^{-i\nu_1(z^*-h)},$$

where $\nu_1=[(S_1/C_D^2)-\frac{1}{4}]^{\frac{1}{2}}$, and h is the "height" of the duct in the log-pressure coordinate. As before, we write $A_1=B_1\mathcal{R}e^{i\theta}$. Complication arises when one tries to apply the lower boundary condition, $w=w_0$ at $z^*=0$, through Eq. (15). As a result, the solutions are not as simple as in the Boussinesq case. The response, for

[4] Note that hydrostaticity was not assumed for the Boussinesq case.

example, becomes [cf. Eq. (7)].

$$I\equiv|\Phi(0)/w_0|=\left(\frac{g}{kC_D}\right)\Big[(\tfrac{1}{4}+\nu_1^2)(1+\mathcal{R}^2)+2\mathcal{R}(\tfrac{1}{4}-\nu_1^2)\cos(2D-\theta)-2\nu_1\mathcal{R}\sin(2D-\theta)\Big]^{\frac{1}{2}}\div\left\{\left[\left(\frac{gH}{C_D^2}-\frac{1}{2}\right)^2+\nu_1^2\right](1+\mathcal{R}^2)+2\mathcal{R}\left[\left(\frac{gH}{C_D^2}-\frac{1}{2}\right)^2-\nu_1^2\right]\cos(2D-\theta)+4\mathcal{R}\nu_1\left(\frac{gH}{C_D^2}-\frac{1}{2}\right)\sin(2D-\theta)\right\}^{\frac{1}{2}}. \quad (17)$$

Eq. (17) can, however, be simplified if one realizes that for the waves we are interested in, the quantity gH/C_D^2 is large (of the order of 100). Dropping terms of order (C_D^2/gH), the denominator of (17) becomes

$$\frac{gH}{C_D^2}\{\epsilon^2+2(1-\epsilon)[1+\cos(2D-\theta)]\}^{\frac{1}{2}},$$

which is the same as the denominator of (7). Thus we can draw the same conclusion as for the Boussinesq case, namely, the response will have maximum peaks of amplitude proportional to $1/|\epsilon|$ if the waves satisfy the quantization given by Eq. (10). The only modification due to compressibility is to replace $N_1\mathcal{H}$ by $S_1^{\frac{1}{2}}h$ in Eqs. (12) and (13). Recognition must also be given to the factor $e^{z^*/2}$ in (16).

3. Ducting by an inversion

In this section we will calculate the reflectivity due to an inversion, modeled by a jump in the mean state

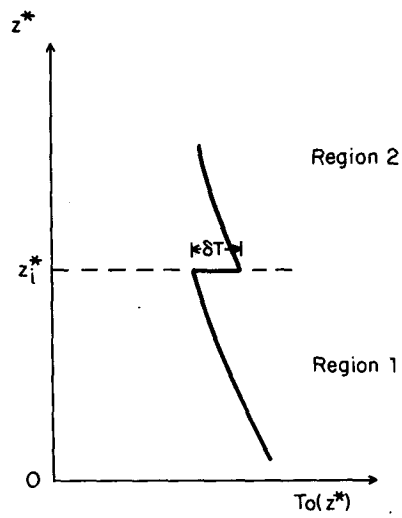

FIG. 2. The temperature structure of the basic state. There is a jump in temperature of δT at $z^*=z_i^*$.

temperature as depicted in Fig. 2. The appropriate equation for a non-isothermal atmosphere is Eq. (16), which in the absence of shear is

$$\frac{d^2}{dz^{*2}}\tilde{w}+\left(\frac{S}{C_D^2}-\frac{1}{4}\right)\tilde{w}=0. \quad (18)$$

The matching condition at the interface $z^*=z_i^*$ is $\tilde{w}$ continuous and $d\tilde{w}/dz^*+RT_0\tilde{w}/C_D^2$ continuous; the latter is obtainable by integrating Eq. (18) across the interface. Assume that the stability is piecewise constant in region 1 and 2, i.e., $S=S_1$ in region 1 and $S=S_2$ in region 2.

The solutions in region 1 can be written as

$$\tilde{w}_1=A_1\exp[i\nu_1(z^*-z_i^*)]+B_1\exp[-i\nu_1(z^*-z_i^*)], \quad (19)$$

where $\nu_1=[(S_1/C_D^2)-\frac{1}{4}]^{\frac{1}{2}}>0$. The solution in region 2 that satisfies the radiation condition is

$$\tilde{w}_2=B_2\exp[-i\nu_2(z^*-z_i^*)], \quad (20)$$

where $\nu_2=[(S_2/C_D^2)-\frac{1}{4}]^{\frac{1}{2}}>0$.

Matching the solutions (19) and (20) across the interface z_i^* gives

$$\frac{A_1}{B_1}=-\frac{[R\delta T-iC_D^2(\nu_2-\nu_1)]}{[R\delta T-iC_D^2(\nu_2+\nu_1)]},$$

where δT is the temperature jump across z_i^*. Thus the reflection coefficient $\mathcal{R}=|A_1/B_1|$ can be expressed as

$$\mathcal{R}^2=\frac{[(R\delta T)^2+C_D^4(\nu_2-\nu_1)^2]}{[(R\delta T)^2+C_D^4(\nu_2+\nu_1)^2]}. \quad (21)$$

We first consider an inversion with a temperature jump but no change in stability. Then

$$\mathcal{R}=(R\delta T)/[(R\delta T)^2+4C_D^4\nu^2]^{\frac{1}{2}},$$

where $\nu^2=S/C_D^2-\frac{1}{4}$.

For a tropospheric lapse rate of 3 K km^{-1}, our stability parameter is about $S=(78\text{ m s}^{-1})^2$. For an inversion strength $\delta T=5$ K, $\mathcal{R}$ is plotted versus C_D in Fig. 3. Note that the reflectivity is quite small for the phase speeds of interest: $\mathcal{R}$ is about 35% for a 25 m s^{-1} wave. As C_D gets smaller, $\mathcal{R}$ approaches 1. However, since small C_D implies short vertical wavelength [see Eq. (12)] these waves are likely to be dissipated.

Incidentally, Eq. (21) can also be used to show that the tropopause is not a good reflector. The reflectivity of a tropopause modeled by a jump in stability (but not in temperature) is

$$\mathcal{R}=\left|\frac{\nu_2-\nu_1}{\nu_2+\nu_1}\right|\approx\left|\frac{S_2^{\frac{1}{2}}-S_1^{\frac{1}{2}}}{S_2^{\frac{1}{2}}\quad S_1^{\frac{1}{2}}}\right|. \quad (22)$$

For $S_2^{\frac{1}{2}}\approx 155$ m s^{-1}, corresponding to a stratospheric potential temperature gradient of 12 K km^{-1}, and $S_1^{\frac{1}{2}}\approx 78$ m s^{-1} we get $\mathcal{R}\approx 33\%$, indicating that the

tropopause is a rather poor reflector. Spurious results are often obtained in numerical models that use the tropopause as a lid.

Eq. (22) provides a motivation for our next section. It seems plausible that if a stable layer is topped by a layer with vanishingly small stability, i.e., $|S_2/S_1| \ll 1$, the reflectivity may approach 1, thus forming a good duct in the stable layer. Unfortunately, such a situation does not occur in reality, because the atmosphere does not have an infinitely thick layer of air with a small stability. However, there still exist synoptic situations where the stability in a *finite* layer can be very small, and sometimes may even become negative if that layer is also saturated with water vapor. These situations will be considered in the next section.

4. Ducting by a conditionally unstable layer

In this section we consider reflections due to an evanescent layer of finite thickness. The calculations are simple and the analysis is essentially the same for both the Boussinesq and compressible atmospheres. For the purpose of presentation, the compressible atmosphere is used. The governing equation is

$$\frac{d^2}{dz^{*2}}y+\nu(z^*)^2y=0, \tag{23}$$

where $\nu(z^*)^2=[S(z^*)/C_D{}^2]-\frac{1}{4}$, and $y=\tilde{w}$.

We take the reflector (viz. Fig. 1, region 2) to be a region where ν^2 is negative, i.e.,

$$-\nu^2=\mu_2{}^2=\frac{1}{4}-\frac{S_2}{C_D{}^2}\gtrless 0. \tag{24}$$

This occurs when the stability in that region is small or negative. For the New England cases discussed by Marks (1975), region 2 corresponds to a layer of convectively mixed air 2.5 km thick. The stability S_2 of that layer of air is vanishingly small due to the elimination of density stratification by the mixing processes. One of the cases discussed by Uccelini—the case of Salem, Ill. (where a duct is expected to exist)—exhibits above the duct a layer ~2.5 km thick with reduced potential temperature gradient *and* very high relative humidity. The effects of moisture saturation on the stability of air have been investigated in a series of papers by Lalas and Einaudi (1973, 1974) and Einaudi and Lalas (1973, 1975). For our purpose here, the main result of their work is that the air is destabilized by the release of latent heat of condensation, and that the value of the actual stability parameter is lower than that of a corresponding layer of dry air (but higher than the value calculated using the wet adiabatic lapse rate). Applying this result, we find that the stability parameter S_2 for this case is slightly negative, and the condition (24) is thus satisfied.

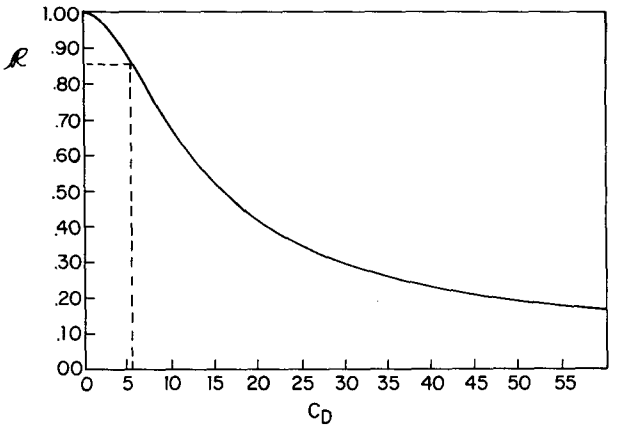

FIG. 3. Reflection coefficient $\mathcal{R}$ versus C_D for an inversion of $\delta T = 5$ K. Note that for $\mathcal{R} \geqslant 85\%$, C_D has to be less than 6 m s^{-1}.

The essential features of the observed atmospheric condition can be simulated by a three-layer model with a lower ducting region, a middle evanescent layer and an upper radiating semi-infinite region. We take $\nu(z^*)^2$ to be piecewise constant, i.e.,

$$\nu(z^*)^2=\begin{cases}\nu_1{}^2 & \text{for } 0\leqslant z^*\leqslant z_1^*: \text{ region 1}\\ -\mu_2{}^2 & \text{for } z_1^*\leqslant z^*\leqslant z_2^*: \text{ region 2}\\ \nu_3{}^2 & \text{for } z_2\leqslant z^*: \text{ region 3}\end{cases} \tag{25}$$

The solutions in regions 1, 2 and 3 can be written, respectively, as

$$\left.\begin{aligned} y_1(z^*)&=A_1\exp[i\nu_1(z^*-z_1^*)]\\ &\quad+B_1\exp[-i\nu_1(z^*-z_1^*)]\\ y_2(z^*)&=A_2\exp(\mu_2 z^*)+B_2\exp(-\mu_2 z^*)\\ y_3(z^*)&=B_3\exp[-i\nu_3(z^*-z_2^*)]\end{aligned}\right\}. \tag{26}$$

The matching conditions across the interfaces are

$$y \text{ and } \frac{d}{dx}y \text{ continuous across } z^*=z_1^* \text{ and } z^*=z_2^*. \tag{27}$$

Applying (27) to (26), we find

$$\mathcal{R}\,e^{i\theta}\equiv\frac{A_1}{B_1}=-\frac{(\sigma\delta-\sigma^*\delta^*e^{-2\mu_2 d})}{(\sigma^*\delta-\sigma\delta^*e^{-2\mu_2 d})}, \tag{28}$$

where $d=z_2^*-z_1^*$, $\delta=\mu_2+i\nu_3$ and $\sigma=\mu_2-i\nu_1$.

If the simplifying assumption $\nu_1=\nu_2$ is made, one obtains

$$\mathcal{R}=\frac{(\mu_2{}^2/\nu_1{}^2)}{[(\mu_2{}^2/\nu_1{}^2)^2+(2\Delta\mu_2{}^2/\nu_1{}^2)^2]^{\frac{1}{2}}}, \tag{29}$$

$$\tan\theta=\frac{2\Delta\mu_2\nu_1}{(\nu_1{}^2-\mu_2{}^2)}, \tag{30}$$

where $\Delta\equiv(1+e^{-2\mu_2 d})/(1-e^{-2\mu_2 d})$.

TABLE 1. Phase speeds (C_D), phase shifts (θ) and reflectivities ($\mathcal{R}$) of the first five modes for the no-shear case.

n	C_D (m s^{-1})	θ	$\mathcal{R}$
0	19.0	0.93	60%
1	7.9	0.50	88%
2	4.9	0.33	95%
3	3.5	0.24	97%
4	2.8	0.19	98%

For the cases in which we are interested

$$\mu_2 d \ll 1 \quad \text{and} \quad (\mu_2^2/\nu_1^2) \ll 1.$$

Consequently, we have approximately

$$\mathcal{R} = \left[1+\left(\frac{2}{\nu_1 d}\right)^2\right]^{-\frac{1}{2}}, \tag{31}$$

$$\tan\theta = \frac{2}{(\nu_1 d)}. \tag{32}$$

Note that the dependence on μ_2 is cancelled out and hence μ_2 does not appear in these equations.

Eq. (31) implies that the quantity $2/(\nu_1 d)$ has to be small for a good reflector. Hence, from (32) one finds that θ is a small quantity for a good duct, verifying the assertion made in Section 2.

For a Boussinesq atmosphere, the quantity $S_1^{\frac{1}{2}}d$ has to be replaed by $N_1\mathfrak{D}$, where $\mathfrak{D}$ is the thickness of the middle layer. Eqs. (31) and (32) become

$$\left.\begin{aligned} \mathcal{R} &\approx \left[1+\left(\frac{2C_D}{N_1\mathfrak{D}}\right)^2\right]^{-\frac{1}{2}} \\ \tan\theta &\approx 2C_D/(N_1\mathfrak{D}) \end{aligned}\right\}. \tag{33}$$

The values for $\mathcal{R}$ and θ for the first five modes are calculated and listed in Table 1, where the values $N_1^2 = 1.3 \times 10^{-4}$ s^{-2}, $\mathfrak{H} = 3$ km and $\mathfrak{D} = 2.5$ km have been used. It is seen that the reflection coefficient for the longest wave ($n=0$ mode) is not large enough to qualify this model atmosphere as a good duct, but it is a significant improvement over that of an inversion. Incidentally, in Table 1 the value of C_D for the $n=0$ mode is not calculated with (13); Eq. (10) has to be used because the assumption of small θ is rather poor due to the low reflectivity.

A spectrograph of the response function I defined in Section 2 is plotted in Fig. 4. Only the first three modes are displayed. It is seen that the $n=0$ mode, represented by a peak at $C_D = 19.0$ m s^{-1}, does not give a pronounced maximum. This is due to the low reflectivity of that mode, as explained in Section 2. In Fig. 4, the value of $N_2^2 = 0$ is used, but the result is very representative of the other cases as long as $\mu_2 d$ is small.

For larger values of μ_2 (i.e., a more unstable layer), the reflectivity of region 2 can be improved (see Fig. 5), and this might increase the reflectivity by 10–20% for the Salem, Ill. case of Uccellini. However, the values of μ_2 that give more acceptable $\mathcal{R}$'s are seldom observed in the real atmosphere. It seems reasonable to conclude that *in the absence of shear, the long lifetimes of the*

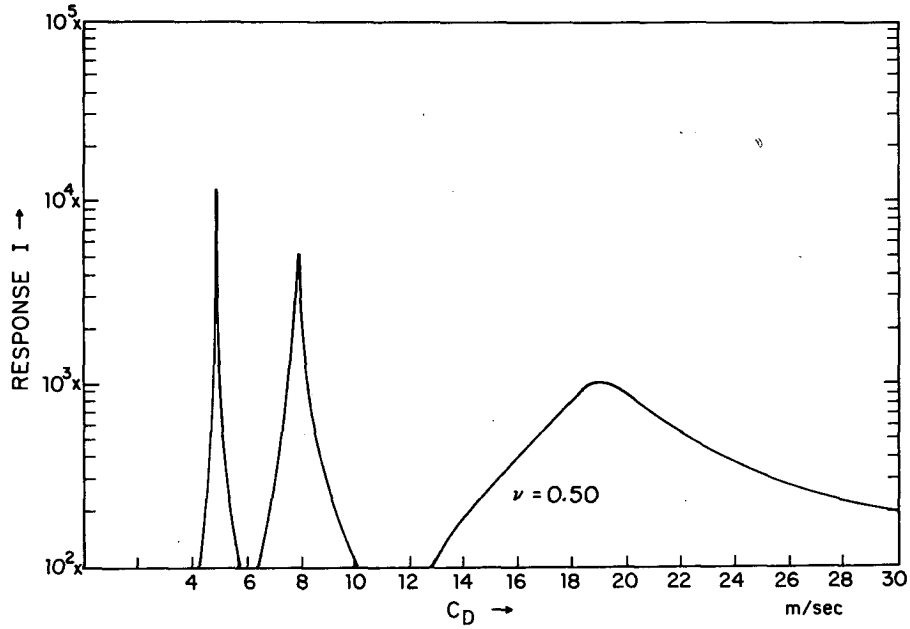

FIG. 4. Spectrogram (response I versus C_D) for the case of ducting by an unstable layer of thickness $\mathfrak{D} = 2.5$ km with no shear.

observed mesoscale waves cannot be explained. For the New England case, one definitely cannot attribute the long (10-cycle) lifetime to ducting due to stability alone. As we shall see in the next section, the story would be completely different if there existed a critical level in the evanescent layer.

5. Ducting by an unstable layer with a steering level

In this section, we consider the ducting due to a sheared layer. Specifically, we shall calculate the reflectivity of an unstable sheared layer (with Richardson number $<\frac{1}{4}$ including negative values) with a critical level imbedded in it. The terms "critical level" and "steering level" will be used interchangeably; both refer to a level where the phase speed of the wave and the unperturbed flow speed are equal. We assume a three-layer model (see Fig. 6) in which the mean wind takes on constant values of $-U$ and U in regions 1 and 3, respectively, and varies linearly in region 2 from $-U$ to U. The Brunt-Väisälä frequency is assumed to be piecewise constant in each layer. We define the Richardson number of the shear layer to be

$$\mathrm{Ri}\equiv N_2^2\Big/\left(\frac{d}{dz}U_0\right)^2=N_2^2\mathfrak{D}^2/(2U)^2. \tag{34}$$

The Taylor-Goldstein equation [(2)] in region 2 becomes

$$\frac{d^2}{dx^2}y_2+\left[\frac{\mathrm{Ri}}{(x-x_c)^2}-1\right]y_2=0, \tag{35}$$

in region 1

$$\frac{d^2}{dx^2}y_1+\lambda_1^2y_1=0,\quad \lambda_1^2=\frac{N_1^2}{k^2(U+c)^2}-1, \tag{36}$$

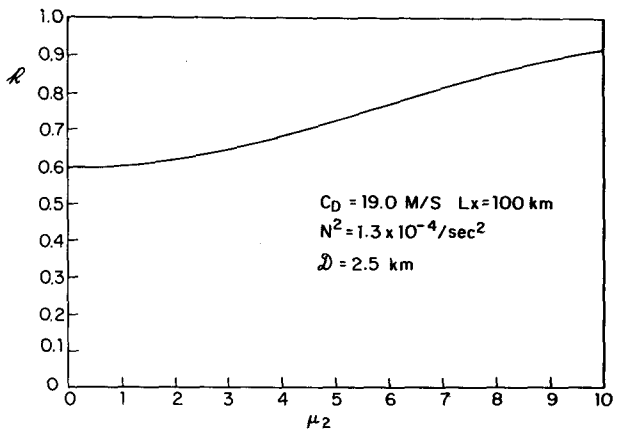

FIG. 5. Reflection coefficient $\mathcal{R}$ versus μ_2.

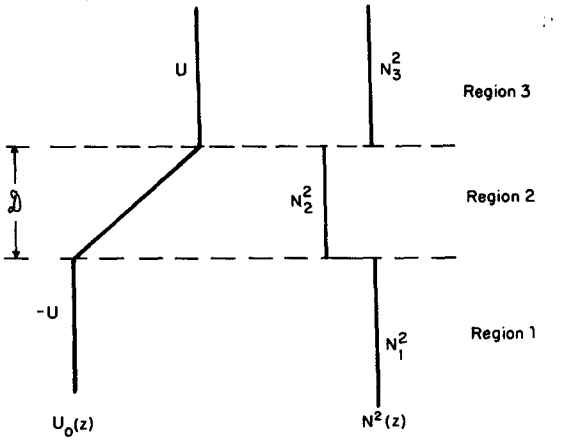

FIG. 6. Schematic diagram of the model atmosphere. Shown are the vertical profiles $U_0(z)$ of the mean wind and the Brunt-Väisälä frequency squared.

and in region 3

$$\frac{d^2}{dx^2}y_3+\lambda_3^2y_3=0,\quad \lambda_3^2=\frac{N_1^2}{k^2(U-c)^2}-1, \tag{37}$$

where $x=kz$, $x_c=c/(dU_0/dz)=\frac{1}{2}c\mathfrak{D}/U$ and $y=w$. The matching conditions across the interfaces $x=x_1$ and $x=x_2$ are

$$y_1=y_2 \quad\text{and}\quad \frac{d}{dx}y_1=\frac{d}{dx}y_2-\frac{1}{x_1-x_c}y_2,\quad \text{at } x=x_1, \tag{38}$$

$$y_2=y_3 \quad\text{and}\quad \frac{d}{dx}y_3=\frac{d}{dx}y_2-\frac{1}{x_2-x_c}y_2,\quad \text{at } x=x_2. \tag{39}$$

The solutions in different regions are

$$\left.\begin{aligned} y_1(x)&=A_1e^{i\lambda_1(x-x_1)}+B_1e^{-i\lambda_1(x-x_1)}\\ y_3(x)&=A_3e^{i\lambda_3(x-x_2)}\\ y_2(x)&=AF(x-x_c)+BG(x-x_c)\end{aligned}\right\}, \tag{40}$$

where $F(x)=x^{\frac{1}{2}}I_\nu(x)$, $\nu=(\frac{1}{4}-\mathrm{Ri})^{\frac{1}{2}}\geqslant 0$, $G(x)=x^{\frac{1}{2}}K_\nu(x)$, I_ν and K_ν being the modified Bessel functions (we have used I_ν and K_ν as independent solutions instead of $I_{\pm\nu}$, which cease to be independent for integer values of ν (cf. Miles and Howard (1964).

There is a branch point in the solutions at $x-x_c=0$. We pick the branch

$$(x-x_c)=(x_c-x)e^{-i\pi} \tag{41}$$

from causality (Booker and Bretherton (1967).

It can be shown that, by matching the Wronskians of the solutions across the interfaces and analytically continuing across the critical level using (41), we obtain the simple relation

$$\lambda_1\{1-\mathcal{R}^2\}=\chi\mathcal{T}^2, \tag{42}$$

where $\mathcal{T}=|A_3/B_1|$ is the "transmission coefficient,"

and

$$\chi \equiv \pi \cos(\nu\pi)[P(\mathfrak{z})^2+\lambda_3{}^2F(\mathfrak{z})^2]+\sin(\nu\pi)[P(\mathfrak{z})Q(\mathfrak{z}) +\lambda_3{}^2F(\mathfrak{z})G(\mathfrak{z})]+\cos(2\nu\pi)\lambda_3, \quad (43)$$

where

$$\mathfrak{z}\equiv x_2-x_c, \quad P(\mathfrak{z})\equiv\frac{d}{d\mathfrak{z}}F(\mathfrak{z})-\frac{1}{\mathfrak{z}}F(\mathfrak{z}),$$

$$Q(\mathfrak{z})\equiv\frac{d}{d\mathfrak{z}}G(\mathfrak{z})-\frac{1}{\mathfrak{z}}G(\mathfrak{z}).$$

Since from (42), one can see that the sign of $\{1-\mathfrak{R}^2\}$ depends critically on the sign of χ, the regions of overreflection and partial reflection can be determined from a consideration of the sign of χ alone. At overreflection, the waves are extracting energy from the mean flow through the critical level, and the lifetime of the waves is affected drastically. Therefore it is important that we first locate the regions of overreflection in the $\nu-c-k$ space.

We note readily that since

$$\lim_{\mathrm{Ri}\to\frac{1}{4}-}\chi=\{\lambda_3+\pi[P(\mathfrak{z})^2+\lambda_3{}^2F(\mathfrak{z})^2]_{\nu=0}\}>0,$$

we have *partial* reflection (i.e., $\mathfrak{R}<1$) as the Richardson number approaches $\frac{1}{4}$ from below. We also note that since

$$\lim_{\mathrm{Ri}\to 0}\chi=-\lambda_3<0,$$

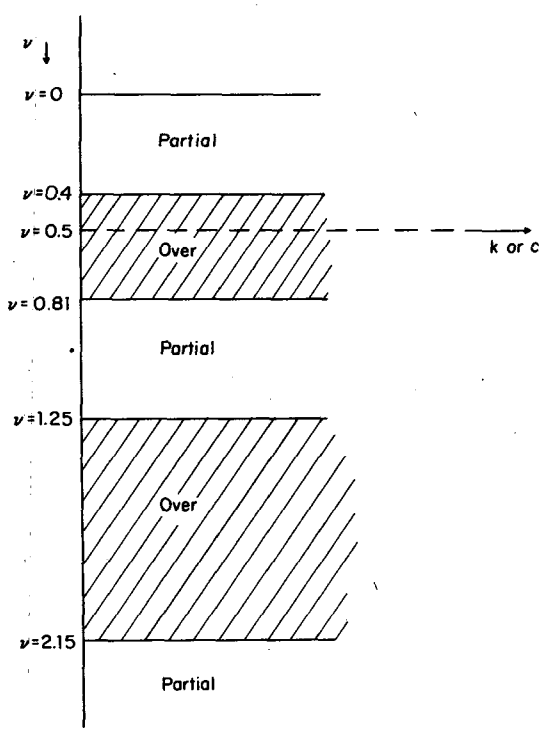

FIG. 7. Regions of partial and over reflections in a $\nu-c$ or $\nu-k$ plane. The overreflection regions are shaded.

we have overreflection (i.e., $\mathfrak{R}>1$) at zero Richardson number. There is a region of transition from overreflection to partial reflection as the Richardson number increases. Jones (1968) has numerically determined that the maximum Richardson number for overreflection is 0.115 for waves which propagate vertically in both regions 1 and 3, while Eltayeb and McKenzie (1975) give a value of 0.1129. However, as can be seen later, this number varies depending on the Brunt-Väisälä frequency in the upper layer.

χ can be numerically evaluated and the results displayed in a three-dimensional parameter space. [For positive Richardson numbers, the results can be found in Jones (1968).] We shall, however, restrict ourselves to mesoscale waves. It can be shown that since for these long waves where $\mathfrak{z}\ll 1$, χ reduces asymptotically to

$$\chi=\frac{1}{2\mathfrak{z}}\mathcal{S}(\nu,\mathfrak{z}_M), \quad (44)$$

where

$$\left.\begin{aligned}\mathcal{S}(\nu,\mathfrak{z}_M)\equiv&\frac{\sin(2\nu\pi)}{\nu}(-\nu^2+\tfrac{1}{4}+\mathfrak{z}_M{}^2)\\ &+2\mathfrak{z}_M\cos(2\nu\pi)\\ \mathfrak{z}_M\equiv&\frac{N_3\mathfrak{D}}{2U}\end{aligned}\right\}. \quad (45)$$

Eq. (44) shows that the sign of χ is determined by the sign of $\mathcal{S}$, which is a much simpler function: it is a function of the Richardson number only (if $\mathfrak{z}_M$ is given) and is *independent of both c and k*, as long a k is small and c is such that a critical level exists. The sign of $\mathcal{S}$ is easily determined and regions of overreflection are plotted in Fig. 7. (We have used $N_3{}^2=1.3\times10^{-4}$ s^{-2}, $\mathfrak{D}=2.5$ km and $U=15$ m s^{-1}.) Note that *a slightly statically unstable shear layer overreflects*. It is also worth noting that for negative Richardson numbers, the regions of overreflection and partial reflection alternate. It can be shown that the reflection coefficient $\mathfrak{R}$ vascillates about 1 and asymptotically approaches 1 as $\mathrm{Ri}\to-\infty$. This point, though interesting, is of academic interest only, and we shall not dwell on it further.

Next we proceed to calculate the reflection coefficient itself. It can be shown, by matching the solutions (40) across the interfaces with (38) and (39), that we have

$$\frac{A_1}{B_1}=\frac{i\lambda_1\alpha+\beta}{i\lambda_1\alpha-\beta} \quad (46)$$

if we let

$$\left.\begin{aligned}a&=-[Q(\mathfrak{z})-i\lambda_3G(\mathfrak{z})]\\ b&=[P(\mathfrak{z})-i\lambda_3F(\mathfrak{z})]\\ \alpha&=aF(\mathfrak{z}')+bG(\mathfrak{z}')\\ \beta&=aP(\mathfrak{z}')+bQ(\mathfrak{z}')\end{aligned}\right\}, \quad (47)$$

where $\mathfrak{z}'=x_1-x_c$. Thus the reflection coefficient is

TABLE 2. Phase speeds (C_D) and reflectivities ($\mathcal{R}$) of the first 11 modes for various ν's [$\nu=(\frac{1}{4}-\mathrm{Ri})^{\frac{1}{2}}$]. Listed are the values of C_D as calculated from the approximate formula (13), and also obtained numerically from the spectrographs.

n	C_D C_D[from Eq. (13)] (m s^{-1})	$\nu=0.4$ C_D[actual] (m s^{-1})	$\mathcal{R}$ (%)	$\nu=0.5$ C_D[actual] (m s^{-1})	$\mathcal{R}$ (%)	$\nu=0.6$ C_D[actual] (m s^{-1})	$\mathcal{R}$ (%)
0	24.8	27.5	99.6	26.0	113	24.5	130
1	8.3	9.0	99.3	9.5	129	9.5	173
2	5.0	5.3	99.4	5.4	117	5.5	129
3	3.5	3.8	99.5	3.8	112	3.8	116
4	2.8	2.9	99.6	2.9	109	2.9	111
5	2.3	2.4	99.7	2.4	108	2.4	109
6	1.9	2.0	99.7	2.0	106	2.0	107
7	1.7	1.7	99.7	1.7	105	1.7	105
8	1.5	1.5	99.8	1.5	107	1.5	105
9	1.3	1.3	99.8	1.3	104	1.3	104
10	1.2	1.2	99.8	1.2	104	1.2	104

given by

$$\mathcal{R}^2\equiv\left|\frac{A_1}{B_1}\right|^2=1-\frac{4\lambda_1\,\mathrm{Im}(\alpha\beta^*)}{|i\lambda_1\alpha-\beta|^2}. \tag{48}$$

It can be proved with some tedious manipulations of Bessel functions that

$$\mathrm{Im}(\alpha\beta^*)=\chi, \tag{49}$$

where χ was given previously by (43). Substituting (49) into (48), one immediately verifies the result that the sign of $\{1-\mathcal{R}^2\}$ is determined by the sign of χ.

The expression (48) is evaluated numerically for different k, c and Ri. The results are somewhat difficult to display. However, for our present purpose only the values of $\mathcal{R}$ at the peaks in response are needed. These are tabulated in Table 2 for a wave whose horizontal wavelength is 100 km. We have chosen three representative values of ν. The first value, $\nu=0.4$, is slightly above the overreflection region (see Fig. 7) and the reflection coefficients are almost 1. As a result, the spectrograph for this case displays sharp pronounced peaks with well-defined modal wave speeds (see Fig. 8). The critical level acts as an almost perfect reflector if ν is near 0.4.

For the values of ν inside the overreflections regime, the wave in the duct is extracting energy from the mean flow. "Lifetime," as defined previously, is no longer a meaningful quantity. In theory, these waves should last indefinitely even in the presence of dissipation. In reality, however, the environmental conditions may not be homogeneous along the wave's path and

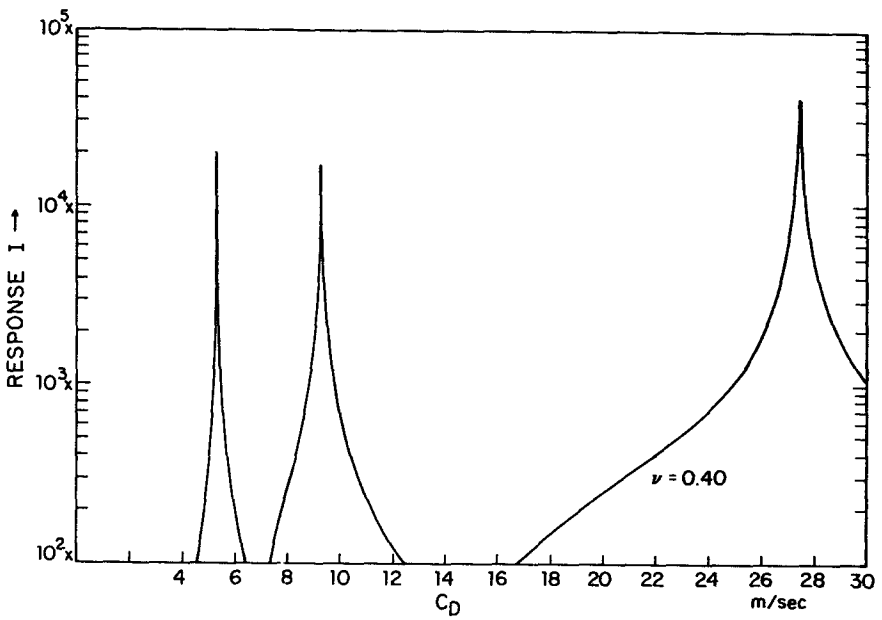

FIG. 8. Spectrogram for the case of ducting by a critical level: $\nu = 0.40$, $\mathfrak{D} = 2.5$ km, $U = 15$ m s^{-1}.

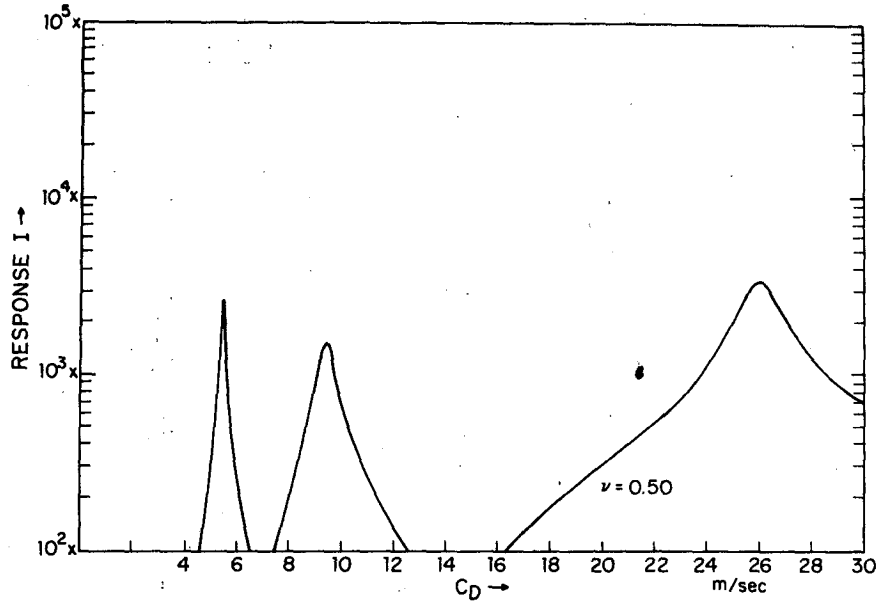

FIG. 9. As in Fig. 8 except for $\nu = 0.50$.

the wave would be dissipated when it moves to a region where it is no longer able to extract energy from the mean flow.

As a direct consequence of our previous result that the *location* of regimes of overreflection is independent of the phase speed, once the Richardson number is within a region of over reflection, *all* wave modes are overreflected. Thus it is possible to observe more than one wave mode in a wave duct. In Fig. 9, the spectrograph for $\nu=0.50$ (Ri=0, overreflecting) is displayed and in Fig. 10 one for $\nu=0.60$ (Ri negative, overreflecting) is also plotted. The fact that the peaks are not as pronounced as in Fig. 8 is merely an indication that these modes are not as close to free neutral solutions as the $\nu=0.4$ case; they would *grow* in amplitude, due to overreflection, if no dissipative mechanism is present. Thus, the width of the $n=0$ peaks in Figs. 9 and 10 does not suggest short lifetimes; however, the lack of sharp selectivity is probably meaningful. It is also found, by numerically evaluating $\mathfrak{A}$ for various values of k, that maximum overreflection typically occurs for smaller horizontal wavelengths

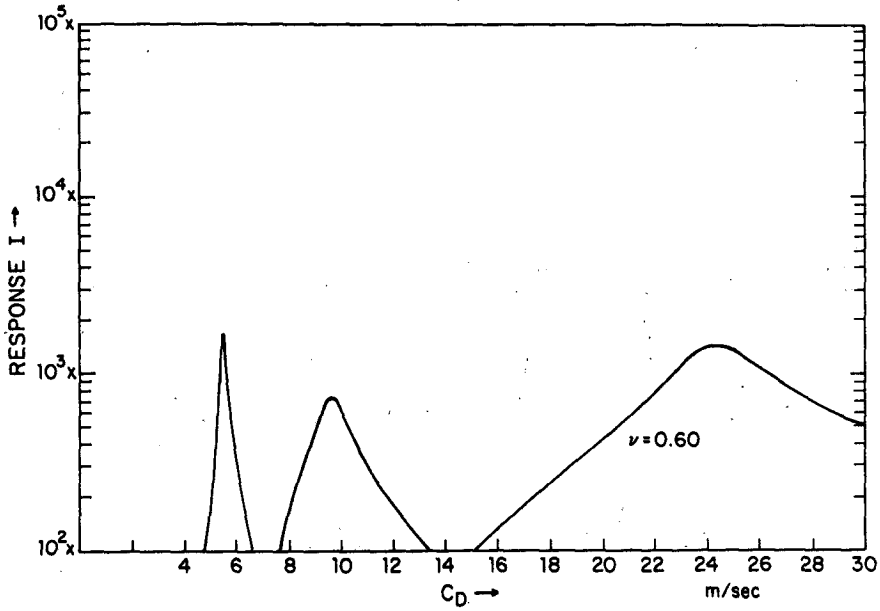

FIG. 10. As in Fig. 8 except for $\nu = 0.60$.

than allowed by our "mesoscale" approximation. Large overreflections are in such instances likely to be associated with the instabilities of the unstable layer rather than the mesoscale organization of such instabilities. The overreflections we obtain in the mesoscale region are generally only slightly greater than 1.

6. Ducting by an unstable layer with shear but without a steering level

Section 5 seems to have given the impression that the existence of a steering level in an unstable layer is a prerequisite for a wave duct. It turns out, with appropriate shears, that a good duct can still be formed without a steering level. From the WKB point of view, the e-folding distance of an evanescent wave in a region of negative N^2 is $\sim[(c-U_0)^2/(-N^2)]^{\frac{1}{2}}$ [see Eq. (2)]. Thus the wave would be severely trapped (i.e., almost totally reflected) if the quantity $(c-U_0)$ is small somewhere in the unstable layer. Intuitively, it seems that the reflection would approach total if $(c-U_0)$ becomes vanishingly small. However, as we have seen in Section 5, when critical level exists such an intuition is not strictly correct: the behavior of the reflection coefficient for negative Richardson numbers is more complicated. This is due to the fact that the WKB notion is not applicable near the singularity when the Richardson number is small. The situation is different for the case where $(c-U_0)$ is small somewhere in the unstable layer *but* never vanishes there. Here the WKB concept is valid because the equation is not singular. This situation is what we shall consider in this section, and we expect to get a good reflectivity for this case.

We consider the same three-layer model as depicted in Fig. 6, except now we assume $c-U_0(z)$ to be positive throughout the three regions.[5] The solutions in regions 1, 2 and 3 are, respectively,

$$\left.\begin{aligned} y_1(x)&=A_1\,e^{i\lambda_1(x-x_1)}+B_1\,e^{-i\lambda_1(x-x_1)}\\ y_2(x)&=AF(x_c-x)+BG(x_c-x)\\ y_3(x)&=B_3\,e^{-i\lambda_3(x-x_2)}\end{aligned}\right\}, \quad (50)$$

where

$$\lambda_1^2=\frac{N_1^2}{k^2(c+U)^2}-1, \quad \lambda_3^2=\frac{N_3^2}{k^2(c-U)^2}-1,$$

and $F(x)=x^{\frac{1}{2}}I_\nu(x)$, $G(x)=x^{\frac{1}{2}}K_\nu(x)$ as before. The matching conditions are the same as (38) and (39).

[5] The case where a steering level exists *above* the unstable layer is similar to this case we are considering, because absorption of waves by a critical level in an upper stable layer is qualitatively equivalent to the radiation condition as far as the wave in the duct is concerned.

If we define $\vartheta_1=x_c-x_1$, $\vartheta_3=x_c-x_2$,

$$a=-[Q(\vartheta_3)-i\lambda_3G(\vartheta_3)],$$
$$b=[P(\vartheta_3)-i\lambda_3F(\vartheta_3)],$$
$$\alpha=aF(\vartheta_1)+bG(\vartheta_1)$$
$$\beta=-[aP(\vartheta_1)+bQ(\vartheta_1)],$$

we obtain an expression similar to (46), i.e.,

$$\frac{A_1}{B_1}=\left(\frac{i\lambda_1\alpha+\beta}{i\lambda_1\alpha-\beta}\right).$$

Therefore the reflection coefficient $\mathcal{R}$ is given by

$$\mathcal{R}=\left|\frac{A_1}{B_1}\right|=\left|\frac{i\lambda_1\alpha+\beta}{i\lambda_1\alpha-\beta}\right| \quad (51)$$

and (51) can be evaluated numerically. However, for our purpose this is not necessary; a simple approximate expression for $\mathcal{R}$ exists for long waves.

For long waves, we have $\vartheta_1\ll1$, $\vartheta_3\ll1$. After doing some asymptotic expansions of Bessel functions for small ϑ_1 and ϑ_3, we obtain, for the case of $N_1^2=N_3^2\equiv N^2$, the following simple formula for $\mathcal{R}$:

$$\mathcal{R}=\left[1+\frac{2\eta}{(1-\eta)^2}\xi\right]^{-\frac{1}{2}}, \quad (52)$$

where

$$\eta=\left[\frac{c-U}{c+U}\right]^{2\nu} \quad \text{and} \quad \xi=\frac{8\nu^2\vartheta_M^2}{(\mathrm{Ri}+\vartheta_M^2)+4\nu^2\vartheta_M^2}.$$

Eq. (52) is well-behaved except at $\mathrm{Ri}\to\frac{1}{4}^-$, where caution must be exercised in taking the limit. The correct limit is

$$\lim_{\mathrm{Ri}\to\frac{1}{4}^-}\mathcal{R}=\left\{1+\frac{4\vartheta_M^2}{(\frac{1}{4}+\vartheta_M^2)^2\left[\ln\left(\frac{c-U}{c+U}\right)\right]^2}\right\}^{-\frac{1}{2}}.$$

From (52), one can see that the reflection coefficient approaches 1^- as $c-U\to0^+$. In Fig. 11, $\mathcal{R}$ [as given by (52)] is plotted for various c and Ri. It is seen that for a wide range of small $c-U$ values, acceptable values of $\mathcal{R}$ can be found. This relaxes the conditions for ducting suggested by Section 5.

7. Summary and comparisons with data

The results of Sections 3–6 permit us to state with some plausibility those conditions under which an effective duct will exist for mesoscale gravity waves. In addition to the stable layer adjacent to the ground (called for by the considerations discussed in Section 2), we require that this layer be capped by another layer wherein the Richardson number is effectively less

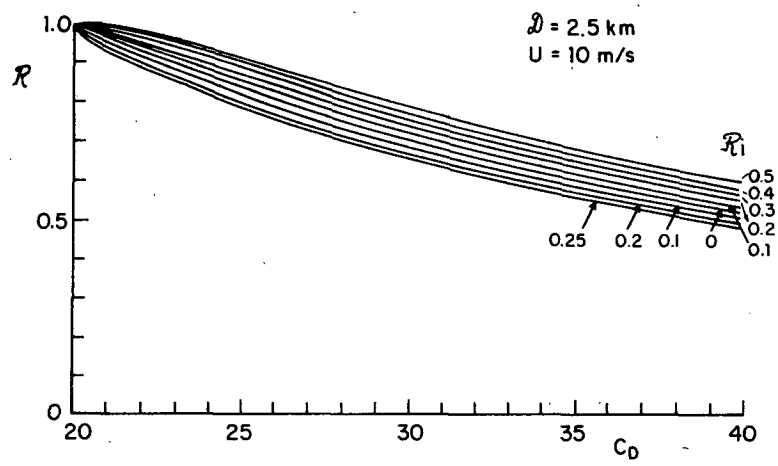

FIG. 11. Reflection coefficient $\mathcal{R}$ versus C_D for the case with shear but no critical level in the unstable region: $U = 10$ m s^{-1}, $\mathcal{D} = 2.5$ km. Shown are various curves for Richardson number Ri ranging from -0.5 to $\frac{1}{4}$.

than $\frac{1}{4}$ because of either of the following possibilities:

1) The layer is sufficiently mixed so that its Brunt-Väisälä frequency is almost zero.

2) The layer is approximately saturated and conditionally unstable so that hydrodynamic perturbations will see a stability due to some mean of the dry and saturated stabilities and hence small or even negative.

In addition, the mean flow within the unstable layer must be such that either of the following hold:

1) There exists some level at which the flow speed equals the phase speed of the ducted mode. This is referred to as a steering or critical level. (Recall that the phase speed of the ducted mode is almost entirely determined by the properties of the stable duct regions.)

2) The flow speed comes very close to the phase speed of the ducted mode. In this case there may be either no steering level at all or the steering level may be above the unstable layer.

Under the above conditions, a ducted mode can exist with little need for forcing. It is of interest to compare these conditions with those existing in observed cases. Fig. 12, from Uccellini (1975), shows the vertical distribution of temperature and relative humidity at two stations through which a mesoscale wave passed. The phase speed of the wave was about 35–45 m s^{-1} relative to the ground (periods were about 3 h corresponding to 400 km wavelengths); unfortunately, no information was given for mean winds though a value of 20 m s^{-1} for near-surface winds is probably reasonable in this case. It is clear from the sounding from Green Bay that the stable region near the ground is much too thin to sustain the observed phase speeds; in addition there is no evidence of a suitably unstable region capping a duct. Indeed, due to the high surface humidity, the bulk of the troposphere was convectively unstable; the wave at Green Bay was, in fact, associated with deep convection and intense precipitation; such situations are ideal for wave-CISK (Lindzen, 1974; Raymond, 1975) wherein there is ample wave forcing and no need for a duct to prevent the loss of wave energy. However, at Salem there was virtually no convective precipitation, and

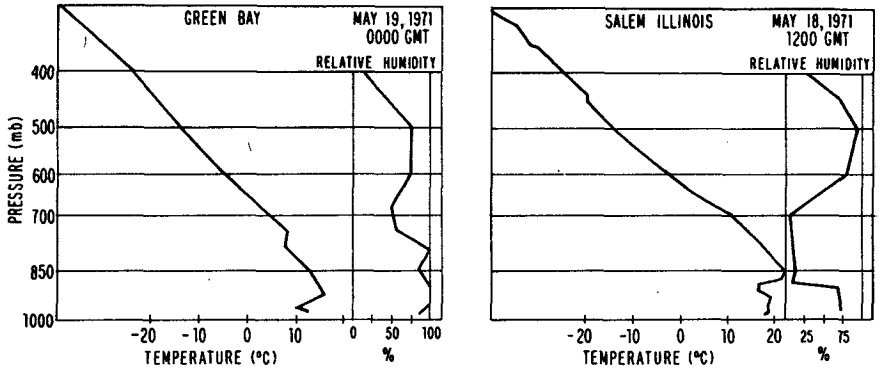

FIG. 12. Vertical distribution of temperature and relative humidity at Green Bay and Salem from Uccellini (1975).

hence no local forcing. Here we find that there is a deep stable layer below 700 mb whose properties are consistent with a 25 m s^{-1} ducted mode, and above we have a nearly saturated conditionally unstable layer. Unfortunately, we have no information as to whether an approximate steering level existed in the unstable region, though the SESAME (1974) report remarks that it is generally observed that waves move in a direction roughly along the mean flow, and that their phase speeds are of the same magnitude as the mean wind. Also in the Midwest, the case studied by Eom (1975) shows a gravity wave occurrence with no closely associated convective activity. The soundings and cross section provided by Eom suggest that a critical level probably exists at around the 500 mb level where the air has a diminished stability due to moisture saturation. The situation for mesoscale disturbances[6] in New England is somewhat clearer. Fig. 13 is a schematic representation of typical conditions associated with mesoscale waves (Marks, 1975). The observed waves have typical phase speeds of 25 m s^{-1} (periods were about 1 h corresponding to wavelengths of about 100 km). The properties of the stable region below 3.6 km are compatible with the observed phase speeds. In addition, the duct is capped by a convectively mixed region containing a steering level. (A detailed examination of the specific cases considered by Marks shows that on occasion the steering level was found just above the convectively mixed layer.)

The above comparisons suggest that mesoscale waves require either conditions propitious to wave-CISK or the presence of a stable duct beneath an unstable region containing a steering level or at least an "almost" steering level.[7]

For a final consistency check, we have obtained from Marks microbarogram data for typical mesoscale waves. These suggest a surface pressure amplitude of 1 mb. Using the equations of Section 2, we find that such a pressure amplitude will be associated with horizontal wind amplitudes of about 4 m s^{-1} suggesting wind changes of 8 m s^{-1} over 30 min. Such changes are indeed characteristic of such mesoscale systems in New England.

8. On the horizontal scale of mesoscale waves

Thus far, nothing in Sections 2–6 serves to explain why mesoscale waves have the scale they have. The properties of the stable duct determine only the phase speed of the mesoscale waves. The instabilities of the unstable layer above the duct are typically characterized by a horizontal scale of the same order as the thickness of the unstable layer—a scale much smaller than that of the mesoscale waves. In Section 1 a hypothesis was put forward to account for the mesoscale based on a similar property of wave-CISK modes (Lindzen, 1974). First, the minimum period over which there can be any collective interaction between convective waves in the stable layer must be $O(2\pi\tau_i)$, where τ_i is a characteristic time scale for the instability. It is intuitively clear that any shorter period would involve changes too rapid to organize convection. Given the phase speed associated with the duct, this minimum period will also determine a minimum wavelength for the mesoscale wave. Our hypothesis is that it is this minimum scale which is indeed realized. In the case of wave-CISK such a scale has the greatest growth rate. Quite possibly a similar argument could be developed for the interaction of convection and ducted waves here.

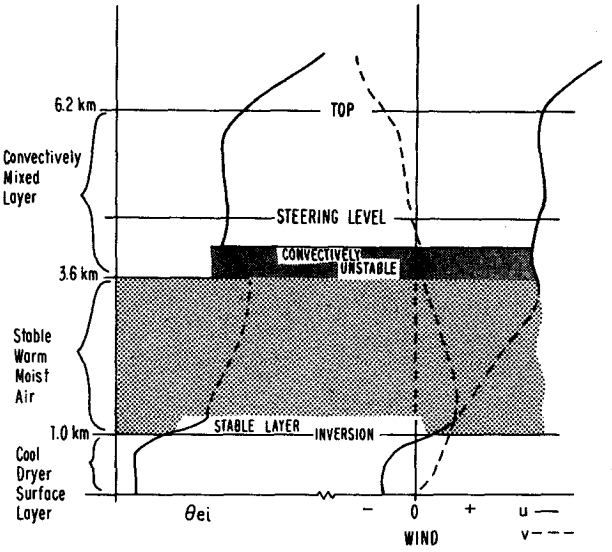

FIG. 13. Schematic representation of typical environmental conditions for mesoscale disturbances from Marks (1975). The equivalent potential temperature (θ_{ei}) profile is on the left and the mean velocity profiles are on the right.

The application of the above argument to the New England disturbances whose period was about 1 h (leading to scales of about 100 km associated with duct phase speeds of about 25 m s^{-1}) suggests a time scale τ_i of about 10 min for the instabilities, which is roughly appropriate to cumulus with a depth of about 2.5 km (see Fig. 13). The waves observed by Uccellini present a slightly more complicated picture. The disturbances observed at Salem probably originated elsewhere where they were associated with cumulonimbus convection. Hence the observed disturbances at Salem should have periods related to the lifetime of cumulonimbi rather than to the lifetime of local instabilities

[6] Here and in subsequent discussions of the mesoscale waves of the New England cases of Marks (1975), we are referring to the mesoscale *precipitation bands*, which we believe are the physical manifestation of the mesoscale *waves*. We will not be concerned with the *coastal fronts*, which were also observed by Marks.

[7] It is interesting to note that wave-CISK instabilities tend to be characterized by vertical wavelengths four times the depth of the moist surface layer. Reference to Fig. 12 then suggests that the wave-CISK modes at Green Bay and ducted modes at Salem could have similar phase speeds.

at Salem. The observed period implies $\tau_i \approx \frac{1}{2}$ h which is a reasonable time scale for cumulonimbi extending about 7 km. That ducted modes can pattern convection in the unstable layer seems reasonable given how delicate a matter the determination of convective plan form is (see Soberman, 1958; Segel, 1966).

The above suggests that when an atmosphere can simultaneously sustain free waves with a phase speed c and convective instabilities with a characteristic time τ_i, then the convection will be patterned with a horizontal wavelength given by

$$L = c \times 2\pi\tau_i. \tag{53}$$

The question now arises as to whether this principle applies to Lamb waves which are the basic free waves of the atmosphere—even when no duct is present [see Lamb (1932), Bretherton (1969) and Lindzen and Blake (1972) for discussion of Lamb waves]; Lamb waves have $c \approx 319$ m s^{-1} (the speed of sound). Although sufficient data are not available to check this point, there are reasons why the answer is probably no. Most significantly the wavelengths implied for $\tau_i \approx 10$ to 30 min are 1000–3000 km; such lengths are typically greater than the extent of convectively unstable layers. However, the situation is different on the sun where a convective layer exists over the entire star. The convective elements are observed as so-called granules having a time scale $\tau_i \approx 3$ to 5 min and a horizontal scale of hundreds of kilometers. The free waves on the sun analogous to Lamb waves have $c \sim$ O (10 km s^{-1}). According to Eq. (53), solar convection should be patterned with a wavelength $\approx$30 000–40 000 km—which is, in fact, the scale of supergranules on the sun [see Leighton (1963) for a review of observational evidence of granules and supergranules].

Acknowledgments. This work has been supported by the National Science Foundation under Grants NSF-GA-DES72-01472-A03 and NSF-ATM-75-20156. Useful conversations with Dr. Pauline Austin, Mr. Frank Marks and Professor Max Krook are also gratefully acknowledged.

APPENDIX

An Estimate of Lifetimes

If the surface above a wave duct is not a perfect reflector, the waves in the duct will gradually lose energy through leakage and hence will not last forever, even if no dissipative mechanisms are present. It seems desirable to have a simple rule of relating the lifetime τ_{lt} of a ducted wave to the reflectivity $\mathcal{R}$ of the surface above the duct. Since wave energy is leaking out of the duct at the rate of $(\overline{p'w'})_1$, the net energy flux out of the duct, we have approximately $\tau_{lt} = \langle E \rangle_1 (\overline{pw'})_1$, where $\langle E \rangle_1$ is the wave energy in a column of air in the duct. Since the energy density in the duct is given by

$$E = \tfrac{1}{2}\rho_0 \left[\overline{u'^2} + \overline{w'^2} + \frac{g^2}{N_1^2} \left(\frac{\overline{\rho'}}{\rho_0} \right) \right],$$

where a bar denotes averaging over a horizontal wavelength,

$$\langle E \rangle_1 = \int_0^{\mathfrak{IC}} E dz = \tfrac{1}{4}\rho_0 \mathfrak{IC} |B_1|^2 \left\{ (\mathcal{R}^2+1)(5\hat{\lambda}_1^2+2) + 2(2-3\hat{\lambda}_1^2)\mathcal{R} \left[\frac{\sin(2D-\theta)}{2D} + \frac{\sin\theta}{2D} \right] \right\}$$

using the solution in Eqs. (3) and (5), with $\hat{\lambda}_1^2 \equiv N_1^2/(k^2 C_D^2) - 1$.

If we are interested only in waves that satisfy the quantization [i.e., Eq. (19)], we can drop the term in brackets in the expression for $\langle E \rangle_1$. The energy flux can be calculated as

$$\overline{(p'w')_1} = \rho_0 \hat{\lambda}_1 C_D |B_1|^2 \{1 - \mathcal{R}^2\},$$

showing that the net flux is upward (leaving the duct) if $\mathcal{R} < 1$.

Since we are interested in a lifetime that is in units of wave cycles, we define $\hat{\tau}_{lt} = kC_D\tau_{lt}/2\pi$ and obtain

$$\hat{\tau}_{lt} = \frac{k\mathfrak{IC}}{4\hat{\lambda}_1}(5\hat{\lambda}_1^2+2)\frac{(1+\mathcal{R}^2)}{(1-\mathcal{R}^2)}.$$

For mesoscale waves $\hat{\lambda}_1^2 \approx N_1^2/(k^2 C_D^2) \gg 1$, we have finally the desired formula

$$\hat{\tau}_{lt} \approx \frac{5(\frac{1}{2}+n)}{8} \frac{(1+\mathcal{R}^2)}{(1-\mathcal{R}^2)},$$

where (13) has been used.

With this simple formula, one can show that, for a wave to last two cycles ($\hat{\tau}_{lt} = 2$), the $n = 0$ mode requires a reflectivity $\mathcal{R} = 85\%$.

REFERENCES

Booker, J. R., and F. P. Bretherton, 1967: The critical layer for internal gravity waves in a shear flow. *J. Fluid Mech.*, **27**, 513–559.

Bretherton, F. P. 1969: Lamb waves in a nearly isothermal atmosphere. *Quart. J. Roy. Meteor. Soc.*, **95**, 754–757.

Einaudi, F., and D. P. Lalas, 1973: The propagation of acoustic gravity waves in a moist atmosphere. *J. Atmos. Sci.*, **30**, 365–376.

——, and ——, 1975: Wave-induced instabilities in an atmosphere near saturation. *J. Atmos. Sci.*, **32**, 536–547.

Eom, J. K., 1975: Analysis of the internal gravity wave occurrence of 19 April 1970 in the Midwest. *Mon. Wea. Rev.*, **103**, 217–226.

Eltayeb, I. A., and J. F. McKenzie, 1972: Critical-level behavior and wave amplification of a gravity wave incident upon a shear layer. *J. Fluid Mech.*, **72**, 661–671.

Jones, W. L., 1968: Reflection and stability of waves in stably stratified fluids with shear flow: A numerical study. *J. Fluid Mech.*, **34**, 609–624.

Lalas, D. P., and F. Einaudi, 1973: On the stability of a moist atmosphere in the presence of a background wind. *J. Atmos. Sci.*, **30**, 795–800.

—— and ——, 1974: On the correct use of the wet adiabatic lapse rate in stability criteria of a saturated atmosphere. *J. Appl. Meteor.*, **13**, 318–324.

Lamb, H., 1932: *Hydrodynamics*, 6th ed. Dover, 738 pp.

Leighton, R. B., 1963: The solar granulation. *Annual Review of Astronomy and Astrophysics*, Vol. 1, Annual Reviews, Inc., 19–40.

Lindzen, R. S., 1974: Wave-CISK in the tropics. *J. Atmos. Sci.*, **31**, 156–179.

——, and D. Blake, 1972: Lamb waves in the presence of realistic distributions of temperature and dissipation. *J. Geophys. Res.*, **77**, 2166–2176.

Marks, F. D., 1975: A study of the mesoscale precipitation patterns associated with the New England coastal front. M.Sc. thesis, Dept. of Meteorology, MIT, 42 pp.

Miles, J. M., and L. N. Howard, 1964: Note on a heterogeneous shear flow. *J. Fluid Mech.*, **20**, 331–336.

Raymond, D. J., 1975: A model for predicting the movement of continuously propagating convective storms. *J. Atmos. Sci.*, **32**, 1308–1317.

Segel, L. A., 1966: Nonlinear hydrodynamic stability theory and its applications to thermal convection and curved flows. *Non-equilibrium Thermodynamics: Variational Techniques and Stability*, Russel J. Donnelly, Ed., The University of Chicago Press, 165–197.

SESAME, 1974: Project Development Plan. NOAA Environmental Research Laboratories, Boulder, Colo.

Soberman, R. K., 1958: Effect of lateral boundaries on natural convection. *J. Appl. Phys.*, **29**, 872–873.

Tepper, M. 1950: A proposed mechanism of squall lines: The pressure jump line. *J. Meteor.*, **7**, 21–29.

Uccellini, L. W., 1975: A case study of apparent gravity wave initiation of severe convective storms. *Mon. Wea. Rev.*, **103**, 497–513.